McGill calibrated colour image database: Details of calibration

1. Aim of this document

The aim of this document is to provide details of how the cameras were calibrated in order to gamma-correct the images and, when required, convert them to LMS cone images. The method of calibration follows that used by Parraga (2003), and we are especially indebted to Alejandro Parraga and Tom Troscianko at the University of Bristol for lending us their facilities and helping with the calibration.

The format of the document is as follows. Section 2 presents the camera settings used when taking the pictures. Section 3 describes the method for colour calibrating the images. Section 4 depicts how the colour calibrated RGB images are converted into LMS cone images. The description of the instruments used in the calibration process is given in Appendix A, and Appendix B provides the Smith & Pokorny (1975) cone spectral sensitivity values used for the RGB to LMS conversion.

Figure 1 indexes the sections in the form of a flow-chart, and summarises the steps involved in the calibration process. The chart also shows the relationship between the sections and the Matlab functions provided on our website.

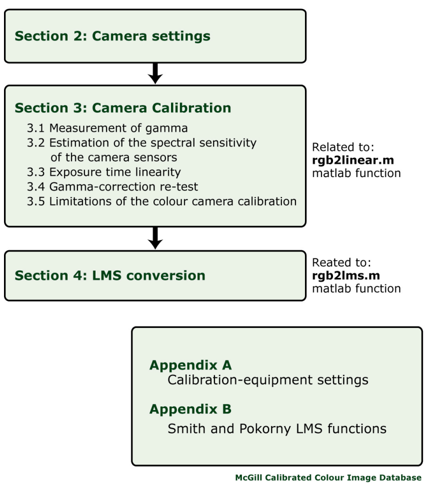

Figure 1. Flow chart of sections and camera calibration.

2. Camera settings

The images in the database were obtained using two Nikon Coolpix 5700 digital cameras, nicknamed “Pippin” and “Merry”. Several parameters were set for all pictures in order to avoid possible artefacts introduced by changes in the depth of field, focal length, etc. Furthermore, the built-in image-processing algorithms (such as image sharpening or noise reduction) were switched off. Table 1 presents the parameters and their settings.

Parameter	Setting	Notes
Resolution	HI (2560 x 1920)	Original image
Format	TIF	No compression
ISO rating	200	Sets the camera sensitivity. Equivalent to an ISP 200 film
Focal length	71.2 mm	
Digital zoom	Off	
White balance	Cloudy	Sets the white color temperature. We selected “cloudy” as it is appropriate for several ambient conditions.
Aperture range	F8	Fixed parameter
Flash	Off	
Mode / Exposure	Aperture priority	The aperture is set to its maximum of F8, which maximises the camera's depth of field, allowing most of the scene to be in focus. With this setting the exposure time is computed by the camera.
Metering	Spot / Matrix	
Saturation	Non / off	
Lens	Normal	
Image sharpening	Non	
Autobraketing	Off	
Noise reduction	Off	

Table 1. Camera settings used to take the pictures in the database.

3. Camera calibration

This section describes how the gammas and spectral sensitivities of the cameras' sensors were measured, and how we gamma-correct the images.

3.1 Measurement of gamma

The function relating the response of each camera RGB sensor to the luminance of the input (the gamma) is not linear. We measured each gamma as follows:

a) The spectroradiometer (SR) was pointed to the central part of each grey square on a Macbeth colour chart illuminated by a constant-current incandescent light source. The luminance of each square was measured and a picture of the square taken.

b) The central part (10 x 10 pixels) of each photographed square was selected and the RGB values averaged. The 10 x 10 pixel-area corresponded approximately to the diameter of the SR aperture.

c) The resulting pixel values were plotted against the Luminance for each square, as shown in Figures 3a and 3b.

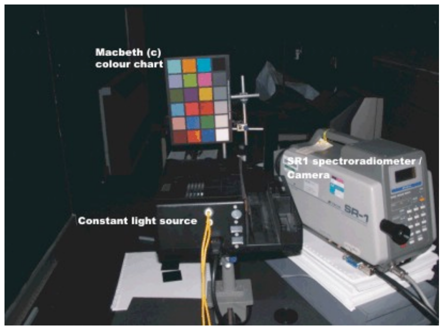

Figure 2. Instruments for gamma correcting the cameras. Dark room, Department of Psychology, University of Bristol.

d) If the luminance *L* is plotted against the pixel value *s*, as in Figures 3a and 3b, the data can be fitted with a gamma function:

$$L = a(b^s + 1), \quad (1)$$

with *a* and *b* being free parameters. *a* is a measure of the slope, or gain of the function and *b* its acceleration. For each camera, a single value of *b* was chosen to give the best overall fit to all three RGB curves:

	Pippin	Merry
b =	1.009696031	1.008634316

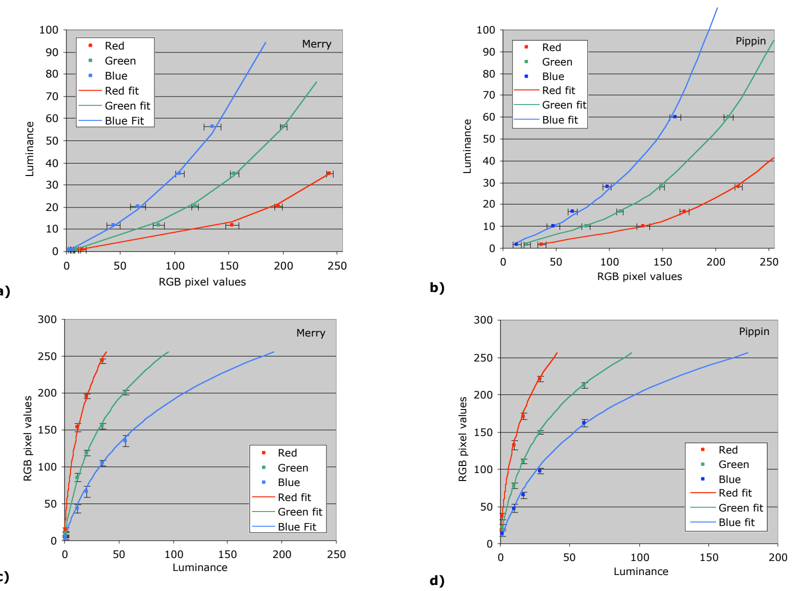

Figure 3. Gammas of the RGB camera sensors. Top figures a) and b): luminance plotted against pixel value; bottom figures c) and d): pixel value plotted against luminance. Left: Merry; right: Pippin.

The gains of the RGB sensors (parameter *a* in Eq. (1)) are set by the 'white balance' option on the camera to produce pictures that look realistic under different lighting conditions (outdoors / indoors). Roughly speaking, with the option set to 'cloudy' (see Table 1) the gains are set such that a neutral grey surface viewed outdoors produces a similar response in all three RGB sensors. However, while natural lighting has on average a flattish spectrum, the incandescent light used in our measurements is heavily weighted towards long wavelengths. If the pixel values are plotted against luminance, as in Figures 3c and 3d, the weighting towards long-wavelengths results in the R>G>B ordering of slopes (in 3a and 3b the ordering of slopes is reversed because luminance is plotted against pixel value).

Given that the incandescent light is not spectrally flat, the gain parameters must be corrected to equalize the RGB responses to a flat spectrum light. In the next section, we will describe how we measured the RGB spectral sensitivity functions, and how we estimated for each sensor the ratio of the response to a flat spectrum light to that of the incandescent light, and how we used this ratio to set the gains (parameter *a* in Eq. (1)).

3.2 Estimation of the spectral sensitivity of the camera-sensors

The cameras' spectral sensitivities within the visible spectrum (400 - 700 nm) were measured using a set of 31 colour filters spanning 400 to 700 nm at 10 nm intervals. A target was placed inside a black box covered in black velvet to avoid reflections. The target consisted of Cyanocrylate adhesive powder (Kodak-Eastman "standard white" with 99% reflectance throughout the visible spectrum). This substance produces a Lambertian (diffuse) pattern of reflected light and has an approximately flat reflectance function across the visible spectrum.

a) The white target was illuminated with a constant light source as shown in Figure 4. A measurement was taken of the central part of the target using the SR at 1 and 10 nm intervals.

b) Each filter was positioned in front of the SR lens and a radiance measurement taken. From the 1 nm interval SR data, we were able to reconstruct the transmitted radiance of the filters and their transmittance. Figure 5 shows the radiance of the incandescent light source reflected from the white target as measured through each filter.

c) A series of pictures of the white target were taken (replacing the SR with the Nikon cameras) through the whole set of colour filters.

d) The RGB pixel values of the centre of each colour-filtered picture where averaged and the exposure time for each picture was recorded.

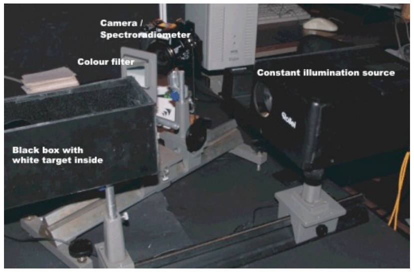

Fig. 4. Instrument set-up for measuring spectral sensitivity. University of Bristol, Department of Psychology dark room.

e) The RGB values, with and without the filters, were gamma-corrected using Eq. (1) with the gain factor *a* set equal for all three sensors, and divided by the recorded exposure time. The value of *a* determined in Section 3.1 was equal to 12.058 for Merry and 8.876 for Pippin.

f) The gamma-corrected RGB values were then divided by the radiance measurements to obtain the RGB sensors' sensitivities at each filter wavelength.

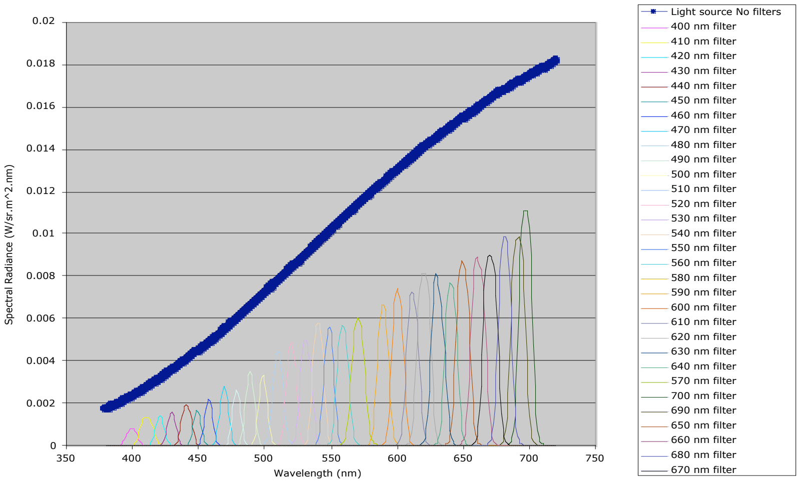

Figure 5. Spectral radiance of the 31 filters in response to the incandescent light source.

g) Using numerical methods, the area under the RGB curves obtained where equalised to produce equal responses to a flat spectrum light. The result it is shown in Figures 6a and 6b.

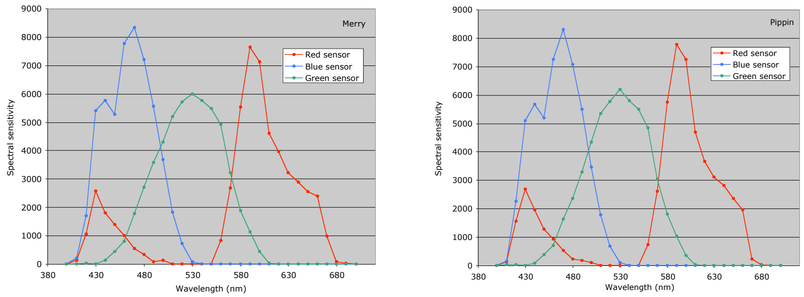

a) **b)**

Figure 6. Spectral sensitivity of the cameras' RGB sensors.

h) In order to compensate for the use of incandescent light instead of white light, the RGB sensitivities (Figures 6a and 6b) were multiplied by the spectrum of the light reflected from the white target (Figure 5). The result is shown in Figures 7a and 7b.

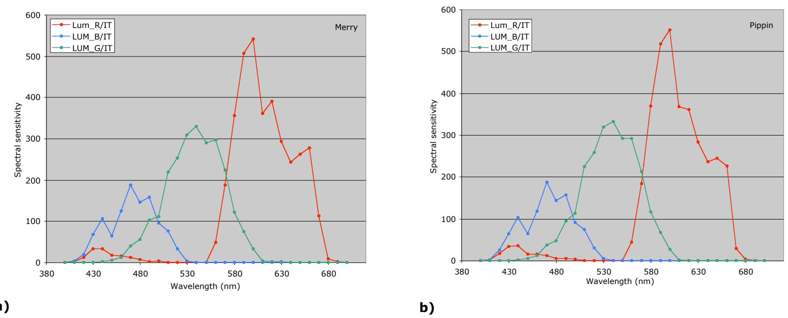

Figure 7. Spectral sensitivities under incandescent light for the cameras' RGB sensors.

i) From Figure 7 we calculated the gain factors (parameter *a* in Eq. (1)) as the ratio of the area under the curve of the green sensor, $\sum G$, to that of the red and blue sensors, $\sum R$, $\sum B$. Thus for the red sensor the parameter *a* in Eq. (1) is computed as

$$a_R = \frac{\sum R}{\sum G}, \tag{2}$$

and for the blue sensor

$$a_B = \frac{\sum B}{\sum G}. \tag{3}$$

Table 2 presents the final set of parameters used for gamma-correcting the images.

Merry				Pippin			
B	a (R sensor)	a (G sensor)	a (B sensor)	b	a (R sensor)	a (G sensor)	a (B sensor)
1.0086343	5.5529104	12.0579051	10.6366886	1.0096960	5.550280693	8.876002262	7.218006459

Table 2. Parameters used for gamma-correcting the images (Eq. (1)); left Merry, right Pippin.

3.3 Exposure time linearity

As mentioned in Section 2, the aperture size for the cameras is fixed and the camera adjusts its exposure time to ensure the picture falls within its dynamic range. For the purpose of gamma-correction we adjusted the RGB values of the images for differences in exposure time under the assumption that the relationship between exposure time and RGB value was linear. Here we test this assumption.

a) A measurement of the light reflected from the central part of the white target was taken using the SR. Neutral density (ND) filters were positioned in front of the SR lens and luminance measurements were taken through each filter.
b) The SR was replaced by the camera. A picture was taken with and without each ND filter.
c) The RGB values of the central part of each picture were averaged and the standard deviation computed.
d) Figures 8a and 8b show log-log plots of the relationship between each camera's output (ordinate) and luminance (abscissa). These values were gamma-corrected with Eq. (1) (using the parameters in Table 2) and divided by the corresponding exposure time of each picture. The coloured lines are the best-fitting linear functions in a log-log space. As can be seen, the slopes of these lines are close enough to unity to assume a linear relationship.

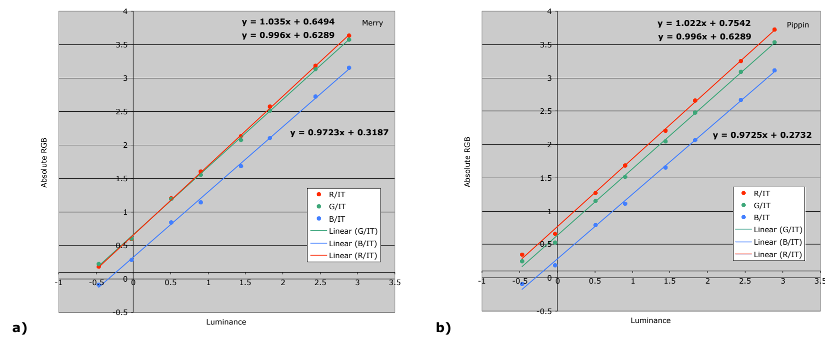

Figure 8. Relationship between RGB values (divided by the exposure time) and luminance (measured by the SR) on a log-log space plot.

3.4 Gamma-correction re-test

Given the importance of gamma correcting the RGB sensors, we decided to run an independent test with different equipment. We constructed a chart of nine Munsell grey-papers, varying in reflectance from black to white. This chart was illuminated with a halogen projector lamp connected to a constant-DC 12V rechargeable battery. The camera was positioned about two metres from the chart, and a micro-photometer (Hanger S1) placed next to the camera. The microphotometer was focused onto a small region in the centre of each paper. A photograph was taken of each paper and the luminance recorded. The camera RGB pixel values were converted using the colour calibration Matlab functions, and divided by the exposure time. Below is plotted the luminance of each piece of paper as a function of the corrected RGB camera values, along with the best-fitting straight lines for each camera sensor.

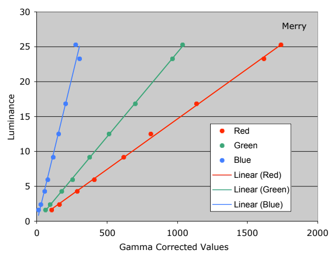

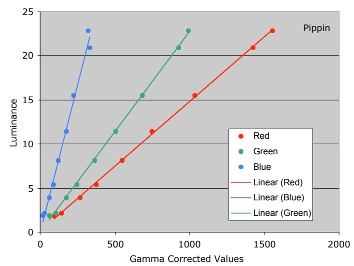

Figure 9. Gamma-correction re-test results for the cameras.

3.5 Limitations of the camera calibration

It is important to note that the cameras' sensors saturate at pixel values below 5 and above 250. Therefore the gamma-corrected values are not valid at these pixel levels.

4. Converting the images from RGB to LMS

The gamma-corrected RGB images can be converted into images that model the responses of the L, M and S cones of the human visual system. For this we use a matrix that transforms the values [R, G, B] into the corresponding values [L, M, S]:

$$[L\ M\ S]' = \mathbf{T} * [R\ G\ B]' \qquad (4)$$

where

$$\mathbf{T} = \begin{bmatrix} t_1 & t_2 & t_3 \\ t_4 & t_5 & t_6 \\ t_7 & t_8 & t_{19} \end{bmatrix}$$

The matrix ***T*** is calculated from the cameras' sensor spectral sensitivities and the Smith and Pokorny (1975) cone sensitivity functions given in Appendix B. The Smith & Pokorny functions were scaled to make them compatible with psychophysical evidence and mathematical constraints. The constraints are as follows:

a) The maximum wavelength sensitivity of the L-M and S-(L+M)/2 mechanisms have to be close to 580 and 506 nm respectively. This means that the value of L(580 nm) must be approximately equal to M(580 nm), and that S(506 nm) should be approximately equal to the combined values of L(506 nm) and M(506 nm).
b) The rows of the transformation matrix ***T*** need to add up to the same number. This is necessary to keep the colour coordinates of a white object the same after the matrix transformation.

Since these two constraints could not be satisfied simultaneously, a compromise was chosen by selecting scale factors that would satisfy the second condition within an error of 2%. Each coefficient of the matrix *T* was obtained as follows:

$t_1 = \Sigma(R_i * L_i)$	$t_2 = \Sigma(G_i * L_i)$	$t_3 = \Sigma(B_i * L_i)$
$t_4 = \Sigma(R_i * M_i)$	$t_5 = \Sigma(G_i * M_i)$	$t_6 = \Sigma(B_i * M_i)$
$t_7 = \Sigma(R_i * S_i)$	$t_8 = \Sigma(G_i * Si_i)$	$t_8 = \Sigma(B_i * S_i)$

* Note that the sum (integration) goes from 400 nm to 700 nm.

Table 3 presents the transformation matrix for the two cameras.

Transformation matrix *T* for the camera Pippin				Transformation matrix *T* for the camera Merry			
	0.428443253	0.495562896	0.075993851		0.431088433	0.494438389	0.074473178
T=	0.243026144	0.614128681	0.142845175	T=	0.245488691	0.614786761	0.139724548
	0.155766424	0.132343175	0.711890401		0.166472303	0.124487321	0.709040376

Table 3. Transformation matrix for the two digital cameras. Refer to Eq. 4.

Appendix A: Calibration-equipment settings

Table 4 presents a list of the objects and instruments used for the camera calibration.

Instruments	Specifications	Description
Spectroradiometer (SR)	Topcon Model SR1	The spectral radiance range is within 380 - 760 nm. The instrument measures spectral radiance, radiance, luminance, tristimulus values (X, Y, Z), chromaticity coordinates (x, y), (u', v'), colour temperature, etc.
Constant illumination source Tugstent-holgen lamp (Osram HLX 64657FGX - 24V, 250W) with a fixed current of 10 amps	DC power supply (Type SP020 - Vinculum products LTD, Royston, Hertz, 0 - 50V, 0-20 amps)	Necessary to avoid variations in the light source produced by fluctuations of the mains during measurement.
Colour chart /ColorChecker	Macbeth (c) chart - Kollmorgen Instruments Corporation	The target for both SR and camera. Consists of 24 squares of different reflectance.
Target	Circular target consisting of Cyanoacrylate adhesive powder stamped on one of the walls of a black box	The white target is similar to the Kodak-Eastman "standard white" with 99% reflectance throughout the visible spectrum. The internal part of the black box was covered in black velvet. Two holes where cut in the box, one opposite the white target and through which the light was projected, the other next to the target through which the measurements were taken.
Colour filters	31 colour filters Ealing Electro-Optics, Watford	Filters spanning from 400 to 700 nm, with peaks at 10 nm intervals.
Neutral density (ND) filters	ND filters of values 0.5, 1.0, 1.5, 2.0, 2.5, 3.0 and 3.5 log units	

Table 4. Objects and instruments used for the camera calibration

Appendix B: Smith and Pokorny LMS functions

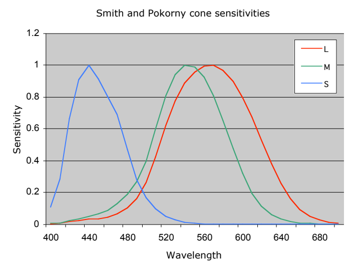

Wavelength (nm)	L	M	S
400	0.002656	0.002823	0.107681
410	0.006889	0.007670	0.284852
420	0.015822	0.018901	0.659235
430	0.023314	0.031709	0.907549
440	0.030096	0.047706	1.000000
450	0.034307	0.063548	0.910458
460	0.041195	0.085998	0.799135
470	0.062656	0.130089	0.689096
480	0.101890	0.188790	0.467724
490	0.161991	0.267030	0.276382
500	0.262851	0.396242	0.163569
510	0.423019	0.594826	0.095565
520	0.616737	0.807756	0.047387
530	0.773215	0.940979	0.025602
540	0.883365	0.996575	0.012414
550	0.953806	0.986529	0.005454
560	0.993322	0.922486	0.002533
570	0.997378	0.806343	0.001445
580	0.964539	0.650729	0.001161
590	0.894190	0.476991	0.000812
600	0.794603	0.317629	0.000610
610	0.670301	0.193308	0.000312
620	0.530066	0.110149	0.000198
630	0.379944	0.058332	0.000090
640	0.256419	0.029558	0.000052
650	0.159030	0.014430	0.000025
660	0.091422	0.006990	0.000014
670	0.048166	0.003330	0.000008
680	0.025667	0.001641	0.000004
690	0.012422	0.000750	0.000002
700	0.006210	0.000368	0.000001

References

Parraga, A. (2003) "Is the human visual system optimised for encoding the statistical information of natural scenes?", PhD Thesis, University of Bristol.

Smith, V. C. & Pokorny, J. (1975) “Spectral sensitivity of the foveal cone photopigments between 400 and 700 nm”. Vision Research, 15, 161-171.